A model investigation of the influence of particle shape on Portland cement hydration

by

J.W. Bullard, E.J. Garboczi
Building and Fire Research Laboratory
National Institute of Standards and Technology
Gaithersburg, MD 20899 USA

Reprinted from Cement and Concrete Research, Vol. 36, pp. 1007- 1015, 2006.

NIST
National Institute of Standards and Technology
Technology Administration, U.S. Department of Commerce

Available online at www.sciencedirect.com
SCIENCE DIRECT
Cement and Concrete Research 36 (2006) 1007–1015
Cement and Concrete Research

A model investigation of the influence of particle shape on portland cement hydration

Jeffrey W. Bullard *, Edward J. Garboczi

Materials and Construction Research Division, National Institute of Standards and Technology, Gaithersburg, Maryland 20899-8615, USA

Received 7 June 2005; accepted 10 January 2006

Abstract

The NIST Virtual Cement and Concrete Testing Laboratory (VCCTL) is used to simulate the influence of particle shape on the hydration kinetics and setting of portland cement. Building on previous work in reconstructing particle shapes from real cements, real-shape particles are used to produce three-dimensional digitized cement paste microstructures, and the hydration of these microstructures is tracked using VCCTL. The degree of hydration and percolation of solids is monitored and compared to experimental data at several water–cement ratios. The simulations predict that shapes of particles influence cement hydration in two ways: the additional surface/volume ratio relative to spherical particles results in greater rates of hydration, and the anisometry in shape influences the degree of hydration at which the particles and hydration products percolate to form a stiff three-dimensional network.
Published by Elsevier Ltd.

Keywords: Hydration; Kinetics; Microstructure; Modeling

1. Introduction

A recent paper [1] demonstrated a mathematical technique for reconstructing and analyzing the three-dimensional (3-D) shapes of cement powder particles extracted from X-ray microtomography data [2]. The technique, originally developed for analyzing the 3-D shapes of aggregates in concrete [3], mathematically models the experimentally acquired shapes using a spherical harmonic (SH) expansion of the particle surface. The shape information of any individual particle can be captured with high resolution by storing only a small number (<500) of coefficients. Using these coefficients, the particle can be reconstructed with arbitrary size, location, and orientation in space.

The availability of real-shape cement particle representations makes it possible to investigate the effects of these shapes on the hydration and setting of cement paste. Cement powders are produced by intergrinding larger clinker and calcium sulfate particles to achieve a desired fineness. Variation in the grinding method, e.g., ball milling versus roller milling, may produce quantitatively different particle shapes, at any given fineness, because the grinding geometry and comminution mechanisms can be different. Additionally, the type and dosage of grinding aids may also influence particle shapes, especially when supplementary cementitious materials are present [4]. Because of these possibilities for varying the shape characteristics of cement particles, it is natural to ask if and how the shape characteristics of cement particles affect the hydration of a cement paste. Spherical shapes have the minimum possible ratio of surface area to volume; the greater the departure from sphericity, the greater this ratio becomes. Therefore, compared to spherical particles, the kinetics of hydration at early ages may be enhanced for pastes formed from non-equiaxed particles. Finally, the setting of cement paste is a percolation phenomenon by which individual cement particles are bridged by hydration products to form a 3-D solid network. The conductivity percolation threshold of a particulate system is known to depend on particle shape [5]. Hence, the solids percolation threshold, and consequently the setting behavior, of a cement paste may also depend on the shape characteristics of its constituent particles.

* Corresponding author.
E-mail address: bullard@nist.gov (J.W. Bullard).

0008-8846/$ - see front matter. Published by Elsevier Ltd.
doi:10.1016/j.cemconres.2006.01.003

Answering these questions experimentally is complicated by the difficulty in controlling particle shape during the grinding process. Analytical models of hydration kinetics, such as the dispersion model of Knudsen [6], cannot provide insights because they are forced to assume spherical particle shapes to make the analysis tractable. Sophisticated numerical models have been reported for simulating the 3-D microstructural development of cement paste as it hydrates [7–9]. However, those models either have not incorporated real particle shapes because they are designed for spherical particles [8,9], or have only incorporated them in two-dimensional versions due to lack of available 3-D shape data [7].

This paper uses the NIST Virtual Cement and Concrete Testing Laboratory (VCCTL) models [10] to examine the influences of particle shape on hydration and setting of cement pastes. The models, hereafter referred to collectively as VCCTL, are an extension of Bentz's CEMHYD3D modeling package [11]. Digitized 3-D cement paste microstructures, differing only in the shape of the particles (spherical versus real shapes), were constructed and their hydration simulated. By tracking the degree of hydration and solid network percolation as a function of time, differences due to particle shape were quantitatively identified.

2. Materials and techniques

VCCTL was used to generate digitized 3-D microstructures of cement pastes formed from the cement CCRL-116, produced as a proficiency sample by the Cement and Concrete Reference Laboratory.[1] CCRL-116 was chosen because its hydration and setting behavior at various water-to-cement (w/c) ratios have been well documented [7,12] and because the characterization data required by VCCTL have been measured [7,12]. Such data include particle size distribution (see Fig. 1), volume and surface area fractions of mineral phases, autocorrelation functions for clinker phases, and total alkali oxide content.

The volume fractions and surface area fractions of the various phases are given in Table 1. These data were obtained by analysis of scanning electron microscope images in combination with X-ray microprobe analysis [13]. The fractions of readily soluble sodium and potassium were not measured directly, but were estimated as 0.03 g Na_2O per gram of cement and 0.33 g K_2O per gram of cement, using the conventions suggested by Taylor [14].

Other than its chemical composition, the surface area of a cement is probably the most important factor influencing its early-age hydration rate. Therefore, it is important to know how closely the computed surface areas of the microstructures generated by VCCTL approximate the experimentally measured value for the cement in question. In this study, the surface area of CCRL-116 was obtained from three different experimental techniques.

The first technique for measuring surface area uses multipoint adsorption isotherms for nitrogen (BET) on a known mass of the powder. The powder was outgassed at 105 °C for 24 h before commencing the adsorption/desorption cycles at different partial pressures of nitrogen in helium. The second technique calculates the surface area from the measured particle size distribution (PSD) of the powder. The PSD measurement is based on scattering of laser radiation from a dilute suspension of the cement particles in isopropyl alcohol. The suspension is dispersed by ultrasonic agitation and then thermally equilibrated prior to the first measurement. Six independent measurements are made on the same suspension. The volume of each particle in the suspension determines the angle-dependent scattered intensity distribution. Mie and Fraunhofer diffraction theories are used to calculate the distribution of particle volumes from the scattered intensity distribution. Particles sizes are given in terms of equivalent spherical diameter, i.e. the diameter of a sphere having the same volume as the actual particle. The estimation of specific surface area from the PSD measurement assumes that the particles are spherical and that they contain no internal porosity. The surface area is normalized by mass using the average specific gravity of the cement.

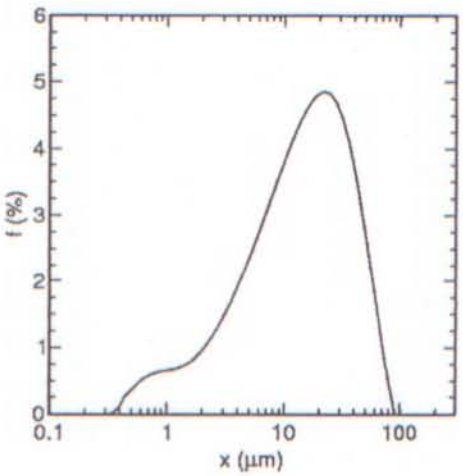

Fig. 1. Particle size probability density function of CCRL-116 as measured by laser diffraction from a dilute suspension of the cement particles in isopropyl alcohol.

The third technique for measuring specific surface area is the Blaine air permeability technique prescribed by the ASTM C204 standard test method [15]. For this method, the value reported in this paper is the average of the values measured by 210 laboratories, as given in the final report on CCRL-116 issued by the Cement and Concrete Reference Laboratory [12].

Particle populations, matching the measured particle size distribution (PSD) of CCRL-116, were randomly placed in a 200^3-voxel box, 1.0 μm/voxel, to produce microstructures with w/c ratios of 0.26 (the value for normal consistency [12,15]), 0.30, 0.40, and 0.50. For the three higher w/c ratios, one microstructure was produced with spherical particles and one was produced with real-shape particles. For w/c=0.26, three statistically identical microstructures of spherical particles, and three statistically identical microstructures of real-shape particles, were generated. For the real-shape particles, equivalent spherical diameters were used to match the PSD of CCRL-116.

[1] Information about the Cement and Concrete Reference Laboratory can be found at http://www.ccrl.us/.

Table 1
Volume fractions and surface area fractions of the four major clinker phases in cement CCRL-116, as measured by SEM/X-ray microprobe analysis

Phase	Volume fraction	Surface area fraction
Tricalcium silicate	0.6708	0.5359
Dicalcium silicate	0.2217	0.3248
Tricalcium aluminate	0.0711	0.1131
Tetracalciumm aluminoferrite	0.0364	0.0261

There is only one cement from which particle shape data have been extracted and analyzed so far [1]: CCRL-133, another proficiency sample cement produced by the Cement and Concrete Reference Laboratory. Although CCRL-133 differs somewhat in mineralogical composition from CCRL-116, an examination of their Blaine fineness ($365\,m^2/kg$ for CCRL-116 and $350\,m^2/kg$ for CCRL-133), and of two-dimensional micrographs of the particles (Fig. 2), suggest that the particle shapes for the two cements are qualitatively similar.

For placing spherical particles, a random parking procedure was used which has been employed previously in numerous studies [7,11,16–18]. For real-shape particles, the spherical harmonic (SH) coefficients for 1005 different particles of CCRL-133, ranging in effective diameter from 15 to 60 μm, were stored in a database. Prior analysis of these particles revealed no systematic correlations between particle volume and shape, as measured by surface-to-volume ratio, aspect ratio, etc. [1]. Therefore, for placing each particle of any desired volume, a particle in the database was sampled at random. The SH coefficients were transformed, using a generalized rotation matrix, through randomly selected Euler angles α, β, and γ to accomplish a random rotation of the particle. A digitized particle of random orientation was produced using the transformed SH coefficients in a series expansion [3], and the SH coefficients were iteratively scaled until the digitized particle volume was within 3% of the desired volume. To match the volume exactly, small numbers of voxels were then attached to, or removed from, random surface sites. The resulting particle was then parked within a 200^3-voxel cube, 1.0 μm per voxel edge, at any randomly chosen location where no overlap with other particles occurred. Since the digitization process forces the loss of some surface detail anyway, only about 200 SH coefficients were used to define each particle.

The smallest particle that can be included by the digitization approach is 1 voxel in size, i.e. 1 μm in diameter. This is an undesirable artifact of digitization because sub-micrometer particles contribute a significant amount of reactive surface area even though they represent a small volume fraction. To compensate for this, sub-micrometer particles are coarse grained as loose clusters having a cluster diameter of 1 μm. An enhanced reactivity is assigned to these clusters due to their excess surface area. The enhancement factor can be calculated unambiguously from the size distribution of sub-micrometer particles, as shown in a recent paper [19]. This coarse-graining assumption therefore correctly accounts for the volume of sub-micrometer particles and their effect on early-age hydration rates. Additionally, the coarse-graining assumption is at least consistent with the fact that small particles tend to flocculate into soft agglomerates due to van der Waals forces. Other artifacts of digitization, and their effect on the present study, are addressed in the Results and discussion section.

Other than the particle placement technique, detailed procedures for reconstructing the phase fractions and distributions in 3-D cement paste microstructures with VCCTL are quite similar to those described elsewhere [7,11,16–18]. Particle microstructures at a given w/c ratio differed only in the gross shapes of particles with minimum diameter of 3.0 μm. The experimental PSD of CCRL-116 (Fig. 1) was discretized into bins, each of which was centered on the odd-integer diameters at which digitized spheres usually are constructed in VCCTL. For real-shape particles, the reconstruction technique can generate a digitized particle of *any* effective diameter, not just odd-integer values. This would represent a significant increase in accuracy of the virtual microstructure. However, for this study, only real-shape particles with odd-integer effective diameters were used to make the closest possible comparison to spherical particles.

VCCTL was used to simulate the hydration and development of each of the microstructures. Saturated conditions were simulated in which the capillary pore water consumed by hydration was continually replenished. The curing temperature

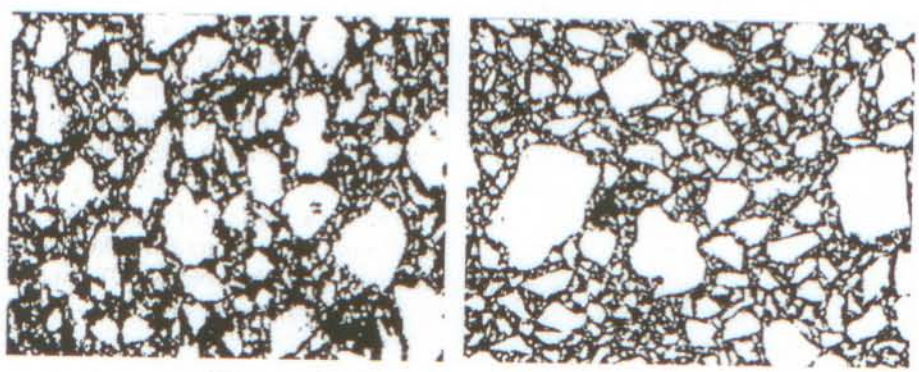

Fig. 2. Two-dimensional cross sections of particles in (a) CCRL-116 and (b) CCRL-133. Both images were acquired by scanning electron microscopy at 500× magnification (256×200 μm field of view). Although the total numbers of particles in the two images differ, the shapes are qualitatively similar in their departure from sphericity.

was assumed constant at 25 °C for the three highest w/c ratios, and at 23 °C for the microstructures with $w/c=0.26$, in accordance with the experimentally measured data. As described previously [7,11], VCCTL maps the number of computational cycles (n) to the age (t) of the paste using the empirical parabolic equation, $t=\beta n^2$. For all the simulations reported here, the time conversion factor β was 3.4×10^{-4} h/cycle^2.

In microstructures generated from random particle placement, the finite size of the system might cause undesirable variation in results between samples. To avoid this, only systems with dimensions of 200 μm in each direction were used. These dimensions have been shown to be large enough to minimize finite size effects for all but the coarsest cements [20]. The absence of significant finite size effects was confirmed in this study by simulating the hydration of six samples at $w/c=0.26$. Three of the samples were composed of spherical particles and three were composed of real-shape particles. Both the degree of hydration as a function of time and the setting behavior were tracked. Within a given microstructure type (spherical or real-shape) the results were reproducible.

3. Results and discussion

3.1. Initial surface areas

Table 2 shows the measured values of specific surface area (SSA) of cement CCRL-116 using each of these three methods described earlier. For the PSD method, two separate samples of powder were measured. Each of these samples was measured six times in the instrument to give an average distribution curve for the sample with very low scatter. The value of SSA reported in the table for this method is the average of the values measured on the two separate samples, and the uncertainty is expressed as plus or minus half the range of those two measurements. For the Blaine method, the value reported is the average of measurements made at 210 laboratories, and the uncertainty is expressed as plus or minus one standard deviation.

The average values of SSA calculated from the PSD exceed that measured by the Blaine method by 24%. An estimate of the uncertainty in the value reported by BET is not available. However, SSA values measured by BET are typically two or three times greater than that measured by the other two methods because nitrogen adsorption measures contributions to the surface area due to surface roughness and any internal porosity that is accessible from the particle surface [21,22]. The PSD and Blaine methods are insensitive to fine-scale surface roughness and internal surfaces of particles, and instead indicate only the gross exterior surface area of the particles. Nevertheless, the discrepancy between the BET value and the other two values is larger than expected and may indicate that some hydration product may have formed on the surface during storage.

Table 2
Comparison of measured specific surface area (m^2/kg) of CCRL-116 cement powder using three different experimental methods: multipoint nitrogen adsorption isotherm (BET), distribution in effective spherical diameter of particles (PSD), and air permeability (Blaine)

Method	Surface area
BET	5270
PSD	448±5
Blaine	365±86

Table 3
Computed surface areas (m^2/g) of microstructures of CCRL-116 generated by VCCTL, using spherical or real-shape particles

Particle shape	$A_{0.30}$ (m^2/kg)	$A_{0.40}$ (m^2/kg)	$A_{0.50}$ (m^2/kg)
Spheres	351	366	381
Real shape	391	417	425

$A_{0.30}$, $A_{0.40}$, $A_{0.50}$, are the specific surface areas computed for $w/c=0.3$, 0.4, and 0.5, respectively.

One way of quantifying the differences in the initial VCCTL microstructures is to compute their SSAs. Table 3 shows the surface areas, in m^2/kg, for microstructures with $w/c=0.30$, 0.4, and 0.5 and composed of either spherical or real-shape particles. Conversion from volume basis to mass basis was made using a specific gravity of 3.15.

The table shows that, as expected, microstructures constructed with real-shape particles have SSAs that are about 12% higher than those constructed using spheres. This additional surface area for digitized real-shape particles is consistent with the average value reported for the excess surface area of a large number of real-shape particles reconstructed by SH expansion from the same data set [1,2].

Table 3 also indicates that the apparent specific surface areas of VCCTL microstructures increase with increasing w/c ratio. As more particles are packed into the same volume to achieve lower w/c ratios, there is an increasing tendency for particle–particle contacts to be formed. In a digital-image format, each interparticle contact eliminates surface area.

Direct comparisons between the computed surface areas of VCCTL microstructures and experimentally measured values are complicated both by the loss of surface area due to interparticle contact in the digital images and by surface artifacts introduced by digitization of the particles. The digitization artifacts are well-known and have been quantified for spherical particles [23]. As for the interparticle contacts, if the loss of surface area due to such contacts is measured on the digital images at $w/c=0.5$, the modified values of specific surface area are 415 and 464 m^2/kg for microstructures made from spheres and real-shape particles, respectively. Again, this is a 12% difference, the same difference as observed previously without digitization. Therefore, although digitization introduces shape artifacts and alters the SSA from the true value, the relative differences in SSA between spheres and real-shape particles are the same after digitization. In addition, the agreement is generally good between VCCTL microstructures and experimental measurements on CCRL-116 using the PSD method (Table 2). Spherical particles underestimate the measured SSA, even though the digitization process adds additional surface area artificially. The reason for the underestimation is likely due to the coarse discretization of the particle size distribution imposed by the model. This PSD discretization has the same influence on real-shape particles as on spherical particles in this

study. And, as mentioned earlier, even more realistic approximations of the measured PSD can be achieved when using real-shape particles.

3.2. Hydration

Fig. 3 shows the simulated development of microstructures of a CCRL-116 paste with w/c ratio of 0.4, using either spherical (left column) or real-shape (right column) particles. From the figure, two qualitative observations can be made. First, not surprisingly, the microstructures comprised of real-shape particles appear more realistic than those made of spheres. The 2-D cross sections of the simulated microstructures of real-shape particles, prior to hydration, appear almost identical to the backscattered electron images obtained experimentally. Second, the details of particle shape become increasingly lost as the particles dissolve and hydration products form in the capillary pore space. In the bottom row of Fig. 3, it is more difficult, but still possible, to distinguish the real-shape particle microstructure from the spherical particle microstructure. This loss of shape information is expected because hydration proceeds by surface reactions (dissolution of unhydrated material and growth of hydration products). Local surface regions with high positive mean curvature on a particle have higher surface-to-volume ratio and will react more rapidly than surface regions on the same particle with lower or negative mean curvature [24]. Hence, particles reacting at their surfaces tend to become more spherical with time. Consequently, any differences in hydration

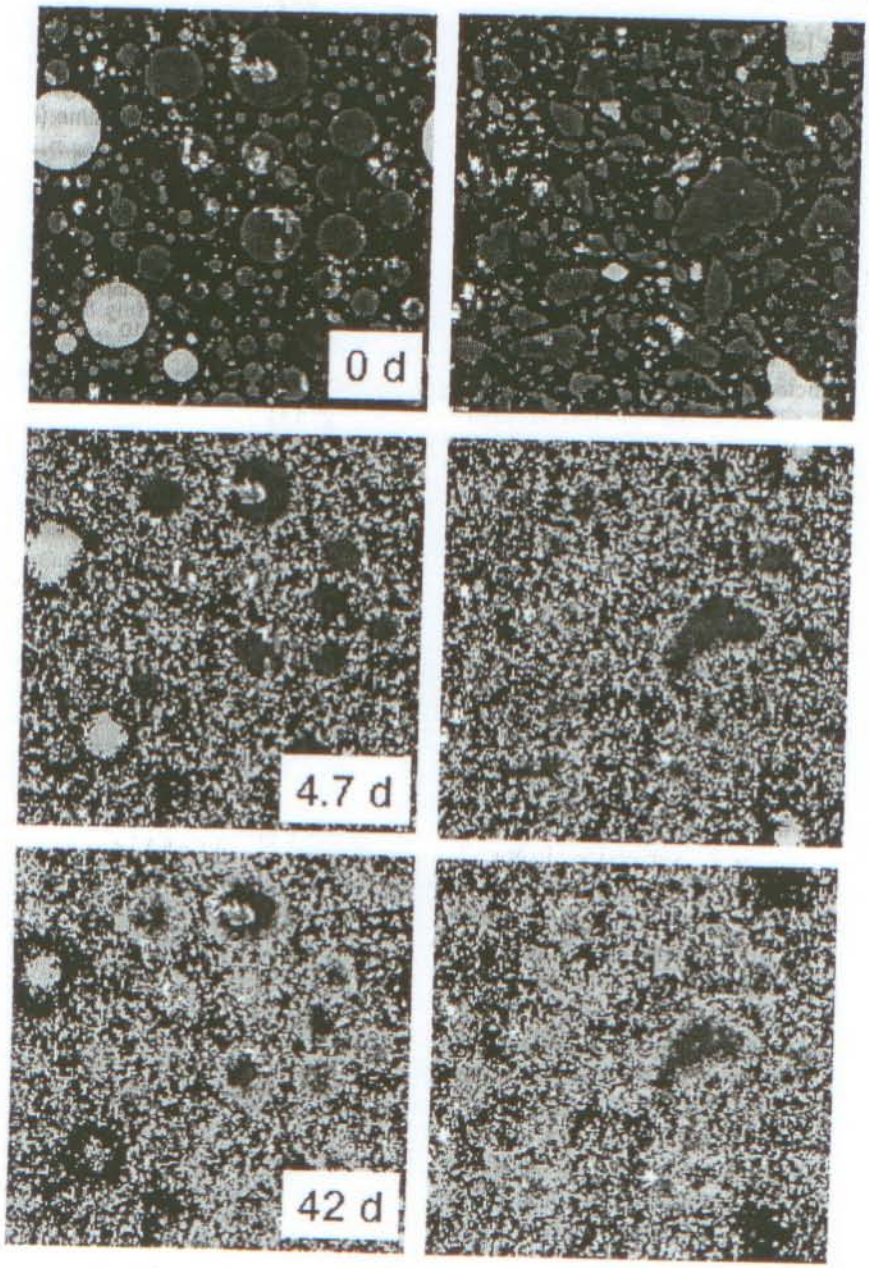

Fig. 3. Two-dimensional cross sections of simulated 3-D microstructures of CCRL-116 with no hydration (top row), 4.7 d of hydration (middle row) and 42 d of hydration (bottom row) at 25 °C under saturated conditions. Spherical particles are shown on the left and real-shape particles on the right. Each image is 200 × 200 μm.

behavior due to particle shape should be most pronounced at early ages, and should lessen with time. Larger particles persist to later ages and their unhydrated cores retain some of the initial shape, as shown in the bottom row of Fig. 3.

Influences of the initially higher surface area of real-shape particles are observed quantitatively when the degree of hydration is examined as a function of age. In Fig. 4, the degree of hydration is plotted against time for real-shape and spherical particle pastes having a w/c ratio of 0.3, 0.4, or 0.5. The predictions—solid or dashed lines for real-shape and spherical particles, respectively—are compared with experimental measurements of the degree of hydration (open circles). The experimental values are measurements of non-evaporable water content relative to the non-evaporable water content at full hydration [25].

At lower w/c ratios (0.4 or less), the capillary porosity in a cement paste depercolates before full hydration is achieved [20]. VCCTL monitors the connectivity of capillary porosity, and the model can be set to automatically switch to sealed conditions when the pore space depercolates [11]. However, there is considerable evidence that switching to sealed curing, although advisable for large masses of paste, often does not fit experimental data as well on smaller laboratory specimens of paste at later ages. For this reason, the results in Fig. 4 were obtained by maintaining saturated curing conditions at all times.

Fig. 4 indicates that at each value of w/c, the degree of hydration at early ages is predicted to be somewhat greater for real-shape particles than for spherical particles. The initial surface area is between 12% and 14% greater for the real-shape microstructures, but the predicted degree of hydration for real-shape microstructures up to 10 h is as much as double that for the spherically shaped microstructures. It should be noted that the increase in surface area should not match the increase in the degree of hydration at any age. Although the initial dissolution rate of unhydrated surfaces is influenced by the surface area in VCCTL, the rates of dissolution and hydration reactions are made to increase nonlinearly as a function of the volume of the C–S–H hydration product formed[2] to simulate the onset of the acceleratory period as an autocatalytic process [11].

Curves for real-shape particles fit the data better than the curves for spherical particles in Fig. 4. However, the fit is sensitive to the value of the time conversion factor β. Increasing or decreasing β will cause the data in Fig. 4 to shift to the right or left, respectively, without altering the shape of the curve. Predictions by VCCTL that relate to kinetics of hydration or microstructural development should be interpreted with the knowledge that the value of β is always chosen a posteriori to provide the best fit to the experimental data. For example, simulations using the spherical-particle microstructures fit the experimental data better than they do in Fig. 4 if $\beta=2.4\times10^{-4}$ h/cycle^2 is used instead of $\beta=3.4\times10^{-4}$ h/cycle^2. In this paper, however, we choose to keep the value of β fixed at 3.4×10^{-4} h/cycle^2 for all simulations so that the differences in predicted hydration kinetics, due only to particle

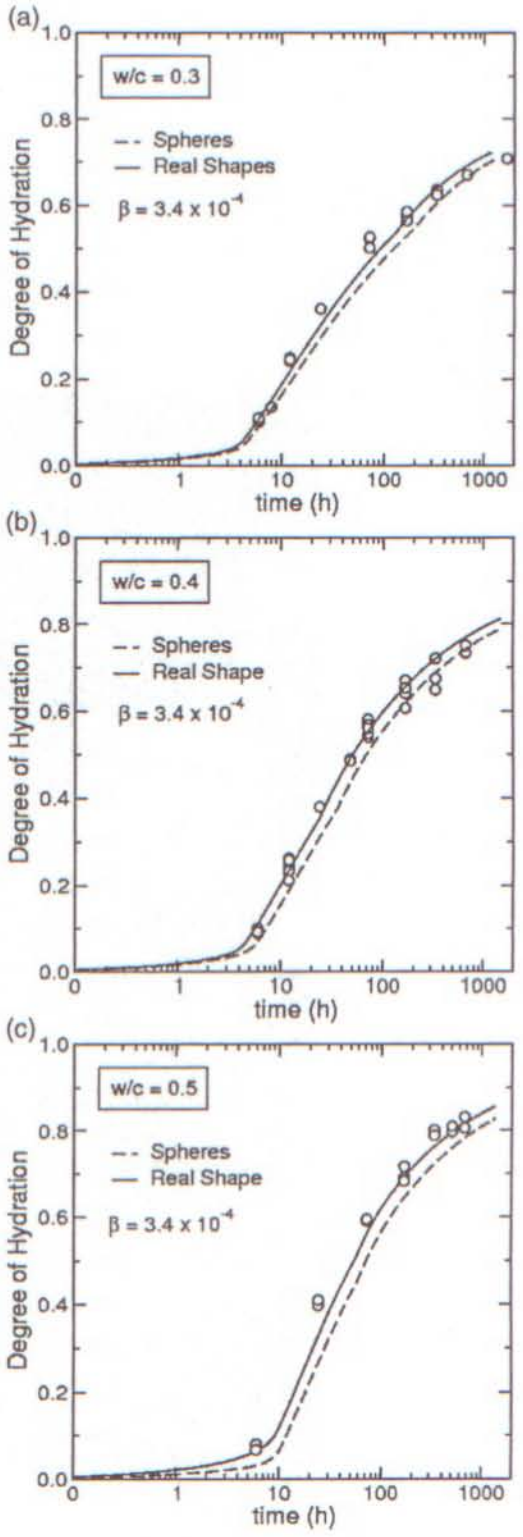

Fig. 4. Predicted and observed degrees of hydration of CCRL-116 as a function of time for (a) $w/c=0.30$, (b) $w/c=0.40$, and (c) $w/c=0.50$. For all simulations, a time conversion factor of $\beta=3.4\times10^{-4}$ h/cycle^2 was used. At each value of w/c, the solid and dashed curves are the predictions for real-shape and spherical particles, respectively, and the open circles are values experimentally measured by non-evaporable water content.

[2] Conventional cement chemistry notation is used, with C = CaO, S = SiO_2, H = H_2O.

shape, can be revealed most clearly. For a given cement, the best-fit value of β often is relatively constant (within 30%) for different w/c ratios and curing conditions [7,26], and this seems to be true in the current study as well, at least over the range of w/c ratios investigated.

3.3. Microstructure development and setting

At least two studies have shown that setting, as measured by the Vicat needle method [15], correlates with the percolation of the solids in 3-D microstructural models of hydration [27,28]. The ASTM method [15] specifies that the initial and final setting times are to be measured on normal consistency (N.C.) pastes. For CCRL-116, the N.C. water value was independently measured at 216 laboratories, with an average of 25.85 (i.e., w/c=0.2585) [12]. Fig. 5 shows the fraction of solids connected as a function of time predicted by VCCTL for a CCRL-116 paste with spherical particles and a paste with real-shaped particles, both of which were created with w/c=0.26. The open circles are predicted values and the error bars indicate the range of values predicted for three statistically identical microstructures. The solid curves are produced to guide the eye. Vertical dashed lines indicate the average experimental values of the initial and final time of set, as measured independently by 208 and 209 laboratories, respectively [12], using the Vicat needle technique described in the ASTM method [15]. For both types of microstructure, the range of values is greatest at the onset of percolation and decreases sharply thereafter, reflecting the sensitivity to microstructural details in finite systems. More generally, in any percolating system, the fluctuations in any measured quantity always are greatest near the percolation threshold [29].

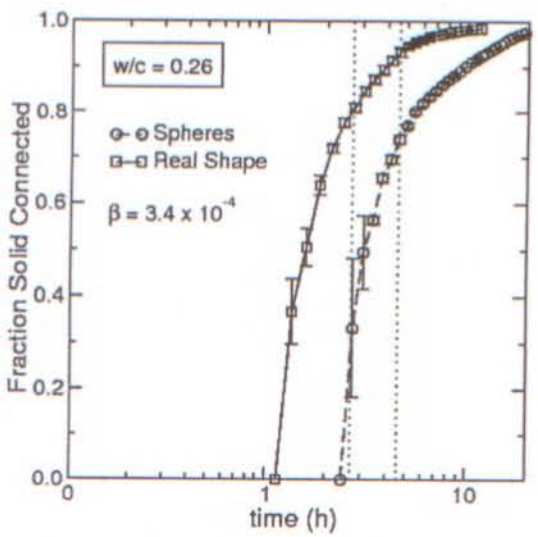

Fig. 5. Volume fraction of connected solids as a function of time predicted by VCCTL for a CCRL-116 cement paste with w/c=0.26, composed either of spherical particles (open circles) or real-shape particles (open squares). The dashed and solid curves are intended as a guide. The vertical lines indicate the experimental initial and final setting times as measured by the Vicat needle method. Error bars indicate the range of values predicted on three statistically identical microstructures of each type.

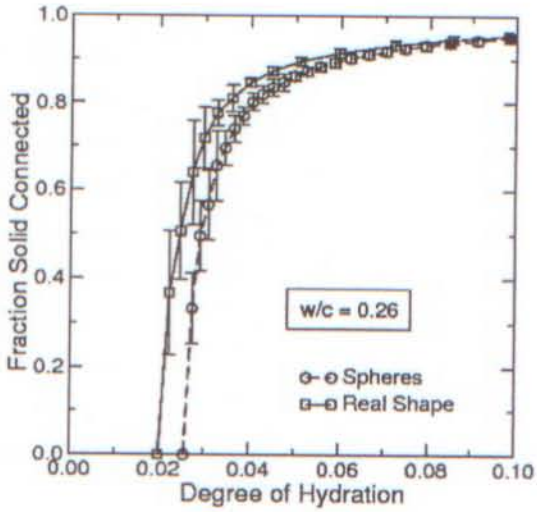

Fig. 6. Volume fraction of connected solids, as a function of the degree of hydration, predicted by VCCTL for a CCRL-116 cement paste with w/c=0.26, composed either of spherical particles (open circles) or real-shape particles (open squares). Error bars indicate the range of values predicted for three statistically identical microstructures of each type, and the dashed and solid curves are intended to guide the eye.

The predicted beginning of set is about 50 min later when spheres are used than when real-shape particles are used (Fig. 5). Even if β is adjusted for spherical-particle microstructures to provide the best qualitative fit to the experimental hydration data in Fig. 4, the predicted setting time is still 35 min later than for real-shape particles. Since the typical range of set times for cements is 2 to 4 h, a difference of 1 h, due solely to differences in particle shape, is significant.

Haecker et al. [27] compared some physical properties predicted by VCCTL to those measured experimentally using pastes made from cement proficiency samples 135 and 141, released in recent years by the Cement and Concrete Reference Laboratory. In that study, initial and final setting times measured by the Vicat needle technique [15] were found to correlate with the predicted connected solid fractions of 0.40 and 0.75, respectively. For CCRL-116, the percolated solid fractions are 0.80 at initial set and 0.92 at final set when real-shape particles are used. For spherical particles, the correlations to initial and final set times are similar to the values previously reported for the other cements modeled by VCCTL using spherical particles [27].

Because the predictions of VCCTL related to kinetics are sensitive to the β value, other comparisons that are independent of kinetics are desirable. Fig. 6 shows, for w/c=0.26 pastes, the volume fraction of solids connected as a function of degree of hydration. Because the figure plots one microstructural quantity as a function of another, it reveals differences in microstructure development which are independent of the rates of hydration. In particular, the percolation of solids in real-shape microstructures occurs with less hydration than it does for microstructures made with spherical particles.

Fig. 6 can be qualitatively interpreted in terms of how percolation thresholds vary with the aspect ratio of particles. Garboczi et al. [5] have shown, for overlapping ellipsoids of

revolution, that the conductivity percolation threshold decreases sharply as the particles become less equiaxed [5]. Hence, at a given volume fraction of solids, microstructures composed of real-shape particles are nearer to percolating than microstructures made from spheres, even prior to hydration. On average, either there are fewer initial gaps between real-shape particles, or the initial gaps are narrower than the gaps between spherical particles at the same volume fraction. Consequently, less hydration product should be required to bridge the gaps between real-shape particles than those between spheres.

3.4. Artifacts introduced by digital imaging

Digital-image modeling of cement microstructure, hydration, and properties has been studied extensively for the last 15 years. The advantages and limitations of the digital-image method are now pretty well understood and have been reported [19,20,30]. Therefore, digitization artifacts will be addressed here only to the extent that they might affect the results of the present study.

First, the resolution limit of the image grid restricts the smallest particles that can be resolved explicitly. In the case of VCCTL, this resolution limit is 1 μm. A coarse-graining approximation [19] has been introduced to minimize the influence of this limitation, as described earlier in this paper. Therefore, a volume of sub-micrometer particles, consistent with particle size distribution measurements, are introduced as clusters with average dimension 1 μm and their enhanced reactivity is included.

Digitization introduces considerable artifacts to the surfaces of particles. For example, in two dimensions a digital circle always has $4/\pi$ times the perimeter of a continuum circle with the same diameter. In three dimensions, a digital sphere always has about 3/2 the surface area of a continuum sphere with the same diameter. This artifact must always be remembered when interpreting the model results. However, in the present study we expect the magnitude of the effect to be essentially the same for real-shape particles and spheres because the real-shape particles have only modest anisometry. Therefore, the results in this study *all* may have systematic error due to the digitization effect, but the *differences* observed between spherical and real-shape particles are still significant.

Percolation phenomena, which are primarily responsible for setting behavior and trends in the transport properties of cement pastes, also have been examined extensively with digital-image models [20,31,32]. The primary effect is that of the resolution of the digital image: percolation thresholds are predicted to decrease significantly with finer resolution. This is due to the ability of finer-resolution representations to detect narrower gaps between particles [20]. Although this is a serious artifact of digitization, the effect should be the basically the same for any microstructure of a given ratio of water to solids. The comparisons in this paper of spheres to real-shape particles should still be valid, despite this artifact, since all the microstructures were created with the same image resolution.

4. Conclusions

The hydration and setting behavior of microstructures made from real-shape particles are predicted by VCCTL to be significantly different from that of spherical-particle microstructures. One reason for the differences is the differences in specific surface area between the two types of microstructure. Less obviously, the geometric differences between real-shape particles and spheres are predicted to influence the microstructure properties at a given degree of hydration. Compared to spheres, the formation of a 3-D percolating network of solids occurs at a lower degree of hydration when real particle shapes are used.

These predicted particle shape effects naturally lead to a consideration of whether it is worthwhile to include real particle shapes in microstructural models of cement paste. For one thing, much of the influence of the increased surface area of real particle shapes can be artificially masked by adjusting the value of the time conversion factor β. Furthermore, the X-ray microtomography measurements required to obtain the 3-D shapes [1] are expensive, as are serial sectioning techniques like those used to visualize the 3-D topology of hydrated cement paste [33] and multiphase metallic alloys [34]. Finally, the computational time required to reconstruct, rotate, digitize, and place real particle shapes is greater than that required to place the same volume of spheres. Therefore, the importance of incorporating particle shape data in simulations should be evaluated based on the phenomena or properties that are of interest.

For modeling the overall kinetics of hydration with VCCTL, the increases in predictive capability may not justify the extra effort required to obtain and use particle shape data. But other properties of cement paste, such as setting time and early-age elastic moduli, are much more sensitive to particle shape [35]. Additionally, recent experiments and simulations of the rheological properties of fresh concrete have demonstrated that the relative viscosity is sensitive to the shape of the coarse aggregate particles [36]. The maximum packing fraction and accompanying rheological properties of cement paste likewise should have the same sensitivity to the shape of cement particles *and* on the progress of hydration reactions. Since all important rheological phenomena are active before set, when the hydration effect of particle shape is most pronounced, the use of real-shape particles will be crucial for understanding and predicting concrete rheology. Therefore, realistic models of cement paste viscosity and yield stress should couple hydrodynamic flow and simultaneous hydration of pastes with real-shape particles.

Currently, little is known about the influences of clinker grinding parameters on particle shape [4]. But as process knowledge increases in this area, it may become feasible to exercise control over particle shape through the choice of grinding method (e.g. roller milling versus ball milling), grinding parameters (e.g., drum speed, type and amount of grinding media), and grinding aids. Once this process knowledge is available, the ability to model hydration of real particle shapes is likely to become important as a design tool to guide the optimization of grinding procedures.

Acknowledgments

The authors thank Dale Bentz and Vanessa Peterson for thoughtfully reviewing the paper and providing valuable comments. Max Peltz is gratefully acknowledged for performing the BET and PSD measurements.

References

[1] E.J. Garboczi, J.W. Bullard, Shape analysis of a reference cement, Cem. Concr. Res. 34 (2004) 1933–1937.
[2] D.P. Bentz, S. Mizell, S.G. Satterfield, J.E. Devaney, W. George, P.M. Ketcham, J.R. Graham, J.E. Porterfield, D.A. Quenard, F. Vallee, H. Sallee, The visible cement data set, J. Res. Nat. Inst. Stand. Technol. 107 (2002) 137–148.
[3] E.J. Garboczi, Three-dimensional mathematical analysis of particle shape using X-ray tomography and spherical harmonics: application to aggregates used in concrete, Cem. Concr. Res. 32 (10) (2002) 1621–1638.
[4] P.C. Taylor, Personal Communication, Construction Technology Laboratories Inc., 2005.
[5] E.J. Garboczi, K.A. Snyder, J.F. Douglas, M.F. Thorpe, Geometrical percolation threshold of overlapping ellipsoids, Phys. Rev., E 52 (1995) 819–828.
[6] T. Knudsen, The dispersion model for hydration of portland cement I. General concepts, Cem. Concr. Res. 14 (1984) 622–630.
[7] D.P. Bentz, Three-dimensional computer simulation of cement hydration and microstructure development, J. Am. Ceram. Soc. 80 (1) (1997) 3–21.
[8] K. van Breugel, Simulation of Hydration and Formation of Structure in Hardening Cement-Based Materials, PhD dissertation, Delft University of Technology, Delft, The Netherlands, 1991.
[9] K. van Breugel, Models for prediction of microstructural development in cement-based materials, in: H. Jennings, J. Kropp, K. Scrivener (Eds.), The Modelling of Microstructure and Its Potential for Studying Transport Properties and Durability, Kluwer Academic Publishers, Dordrecht, The Netherlands, 1996, pp. 91–106.
[10] J.W. Bullard, The virtual cement and concrete testing laboratory consortium annual report 2003, NISTIR, vol. 7096, U.S. Department of Commerce, 2004.
[11] D.P. Bentz, "CEMHYD3D: A three-dimensional cement hydration and microstructure development modeling package. Version 3.0." NISTIR 7232, U.S. Department of Commerce. Available at http://ciks.cbt.nist.gov/monograph, 2005.
[12] Final Report: Portland Cement Proficiency Samples Number 115 and Number 116, Cement and Concrete Reference Laboratory, 1995.
[13] D.P. Bentz, P.E. Stutzman, C.J. Haecker, and S. Remond, "SEM/X-ray imaging of cement-based materials," in Proceedings of the 7th Euro-seminar on Microscopy Applied to building Materials, H. S. Pietersen, J. A. Larbia, and H. H. A. Janssen, editors, pp. 457–466, Delft University of Technology, 1999. Available online at the NIST electronic monograph, http://ciks.cbt.nist.gov/monograph, Part I, Chapter 4, Section 1.
[14] H.F.W. Taylor, A method for predicting alkali ion concentrations in cement pore solutions, Adv. Cem. Res. 1 (1987) 5–16.
[15] Annual Book of ASTM Standards, vol. 04.01, ASTM International, West Conshohocken, PA, 2000.
[16] D.P. Bentz, E.J. Garboczi, C.J. Haecker, O.M. Jensen, Effects of cement particle size distribution on performance properties of cement-based materials, Cem. Concr. Res. 29 (1999) 1663–1671.
[17] D.P. Bentz, O.M. Jensen, K.K. Hansen, J.F. Olesen, H. Stang, C.J. Haecker, Influence of cement particle size distribution on early age autogenous strains and stresses in cement-based materials, J. Am. Ceram. Soc. 84 (1) (2000) 129–135.
[18] D.P. Bentz, X. Feng, C.J. Haecker, P.E. Stutzman, "Analysis of CCRL proficiency cements 135 and 136 using CEMHYD3D," NISTIR 6545, U.S. Department of Commerce. Available online at the NIST electronic monograph, http://ciks.cbt.nist.gov/monograph, Part I, Chapter 4, Section 3, 2000.
[19] J.W. Bullard, "Coarse-graining approximation for simulating surface reaction kinetics in particulate systems," Comput. Mater. Sci. (in press).
[20] E.J. Garboczi, D.P. Bentz, The effect of statistical fluctuation, finite size error, and digital resolution on the phase percolation and transport properties of the NIST cement hydration model, Cem. Concr. Res. 31 (2001) 1501–1514.
[21] H.F.W. Taylor, Cement Chemistry, 2nd edition, Thomas Telford, London, 1997.
[22] T. Allen, Particle Size Measurement, 5th edition, Chapman and Hall, New York, 1997.
[23] E.J. Garboczi, D.P. Bentz, N.S. Martys, Digital images and computer modelling, in: P.z. Wong (Ed.), Methods in the Physics of Porous Media, Experimental methods in the Physical Sciences, vol. 35, Academic Press, San Diego, CA, 1999, pp. 1–41.
[24] J.W. Bullard, Digital-image-based models of two-dimensional microstructural evolution by surface diffusion and vapor transport, J.Appl. Phys. 81 (1) (1997) 159–168.
[25] K.A. Snyder, D.P. Bentz, Suspended hydration and loss of freezable water in cement pastes exposed to 90% relative humidity, Cem. Concr. Res. 34 (11) (2004) 2045–2056.
[26] D.P. Bentz, A three-dimensional cement hydration and microstructure program: I. Hydration rate, heat of hydration, and chemical shrinkage, NISTIR, vol. 5756, U.S. Department of Commerce, 1995.
[27] C.J. Haecker, D.P. Bentz, X.P. Feng, P.E. Stutzman, Prediction of cement physical properties by virtual testing, Cem. Int. 1 (3) (2003) 86–92.
[28] A. Princigallo, P. Lura, K. van Breugel, G. Levita, Early development of properties in a cement paste: a numerical and experimental study, Cem. Concr. Res. 33 (7) (2003) 1013–1020.
[29] D. Stauffer, A. Aharony, Introduction to Percolation Theory, 2nd edition, Taylor and Francis, London, 1994.
[30] J.W. Bullard, E.J. Garboczi, W.C. Carter, J. Edwin, R. Fuller, Numerical methods for computing interfacial mean curvature, Comput. Mater. Sci. 4 (1995) 103–116.
[31] D.P. Bentz, E.J. Garboczi, Percolation of phases in a three-dimensional cement paste microstructure model, Cem. Concr. Res. 21 (1991) 325–344.
[32] E.J. Garboczi, D. Bentz, Computer simulation of the diffusivity of cement-based materials, J. Mater. Sci. 27 (1992) 2083–2092.
[33] P.E. Stutzman, Backscattered electron imaging of serial sections of hydrated cement paste, Advances in Cementitious Materials, Ceramic Transactions, vol. 16, American Ceramic Society, Westerville, OH, 1990, pp. 237–249.
[34] J. Alkemper, P.W. Voorhees, Quantitative serial sectioning analysis, J. Microsc. 201 (2001) 388–394.
[35] C.J. Haecker, E.J. Garboczi, J.W. Bullard, R.B. Bohn, Z. Sun, S.P. Shah, T. Voigt, Modeling the linear elastic properties of portland cement paste, Cem. Concr. Res. 35 (2005) 1948–1960.
[36] R.J. Flatt, N. Martys, L. Bergstrom, The rheology of cementitious materials, MRS Bull. 29 (5) (2004) 314–318.